ELSEVIER

Journal of Biomechanics 40 (2007) 86–91

JOURNAL OF BIOMECHANICS

www.elsevier.com/locate/jbiomech
www.JBiomech.com

A kinematic model of the shoulder complex to evaluate the arm-reachable workspace

N. Klopčar*, M. Tomšič, J. Lenarčič

Jožef Stefan Institute, Jamova 39, 1000 Ljubljana, Slovenia

Accepted 15 November 2005

Abstract

Upper-arm evaluation including shoulder motion in physiotherapy has no three-dimensional tool for an arm-functioning evaluation, which hampers an uniform, objective comparison. Human shoulder complex models suffer from lack of shoulder girdle kinematic data. A kinematic shoulder-complex model with six degrees of freedom is proposed as the composition of the inner joint representing the shoulder-girdle joints and outer joint representing the glenohumeral joint. The outer shoulder joint has three perpendicular rotations: adduction/abduction, retroflexion/flexion and internal/external rotation of the humerus. The inner shoulder joint has two rotations, depression/elevation and retraction/protraction, and one translation, which are all dependent on the elevation angle of the humerus. The human arm-reachable workspace that represents the area within reach of the wrist is calculated on the basis of the shoulder-complex model and the additional elbow-joint direct kinematics. It was demonstrated that cross-sections of the calculated workspace are in agreement with the measured arm-reachable workspace in all three anatomical planes. The arm-reachable workspace volume and graphics were calculated and a comparison of the arm's workspaces during a patient's shoulder treatment was made. The obtained numerical and graphical arm-reachable workspaces can be used for arm-functioning evaluations in rehabilitation and ergonomics.

Keywords: Shoulder complex; Shoulder girdle; Kinematics; Arm model; Workspace

1. Introduction

The kinematics of the human shoulder complex involves complicated movements that do not have a fixed center of rotation (Doorenbosch et al., 2001). This complexity is the main reason for introducing the simplification in which the shoulder girdle (SG) is neglected, i.e., the shoulder complex is simply treated as a glenohumeral joint with three serial rotational joints. The SG joints have a small working space in comparison to the glenohumeral joint; however, SG contribution as the inner link is important. It helps the arm to avoid the trunk during movements and brings redundancy to the arm system.

*Corresponding author. Tel.: +386 41 933 078; fax.: +386 423 22 09.
E-mail address: nives.klopcar@ijs.si (N. Klopčar).

0021-9290/$ - see front matter
doi:10.1016/j.jbiomech.2005.11.010

Here, upper-arm refers to the part of the arm from the sternum to the wrist. All the wrist positions in space are defining the arm-reachable workspace (ARW) that visualize the upper-arm functioning. In a three-dimensional (3D) mathematical model of the shoulder complex (Engin and Tümer, 1989) it seems that the shoulder's sinus cone limits are the complete information for the ARW (Engin and Peindl, 1987). However, the ARW is not spherical inside these limits. Therefore, the model has to include the movement relations between the segments of the shoulder complex.

The anatomical properties of the shoulder complex do not directly correspond to the arrangement of simple rotations around fixed axes (Dvir and Berme, 1978). The axial range of motion of the humerus depends on its position in the shoulder sinus cone, where the minimal and maximal range of rotation varies (Wang et al., 1998). Therefore, the interdependencies between the joint coordinates for the glenohumeral joint (Lenarčič and Umek, 1994) and the SG joints (Klopčar and Lenarčič, 2005) have to be included in the model of the shoulder complex.

Human reaching tasks in a 3D environment are an important issue for shoulder-complex simulations, animations, rehabilitation and the design of an ergonomic working environment. The recent, 3D musculoskeletal models of the shoulder and elbow for dynamical simulation (van der Helm, 1997; Maurel and Thalmann, 2000) are very exact. They can calculate forces and moments in defined arm positions. In this study we are searching for all the arm positions that can be reached, which is why a kinematic upper-arm model is sufficient.

The above-mentioned measurements and models are computationally expensive for modern computer applications that calculate the total ARW. The purpose of this upper-arm model is an interactive computation of the ARW. In order for it to be of use as an assistant tool, the upper-arm model has to be based on the input data of the shoulder's range of motion (RoM) that are already in common clinical use. They contribute 40% to the clinical method of functional assessment of the shoulder (Constant and Murley, 1987). On the other hand, the kinematic model is sufficient when it calculates the exact ARW, which is in agreement with the measured wrist reach in the main anatomical planes.

The purpose of this study is to present an assistive tool for evaluating shoulder pathologies with an ARW. It offers a new graphical and numerical expression of the shoulder's functioning and is easily understood by patients and professionals engaged in a clinical evaluation of the upper-arm. An example of the rehabilitation of a patient with a frozen shoulder is used to demonstrate its applicability and advantages.

2. Materials and methods

2.1. Range-of-motion measurements for the upper-arm model

The shoulder's RoM is measured as inclinations in each anatomical plane during active or passive arm elevation in terms of the arm's reference position. As Norkin and White (1985) defined: the shoulder elevation through retroflexion (φ_{Fmin}) and flexion (φ_{Fmax}) are measured in the sagittal plane; the elevation through adduction (φ_{Amin}) and abduction (φ_{Amax}) are measured in the frontal plane; the internal (φ_{Rmin}) and external rotations (φ_{Rmax}) are measured in the horizontal plane. The principal elbow movements are extension (φ_{EFmin}) and flexion (φ_{EFmax}), measured in the sagittal plane (Fig. 1). This is a standard goniometric measurement technique to determine the extent of a shoulder injury in physiotherapy (Constant and Murley, 1987). In the present study the measured shoulder RoM declinations are defined as the minimum and maximum values in a specific plane regarding to the initial position of the humerus. In this way, the shoulder's RoM was measured (Table in Fig. 2) on the healthy right arm of a 25-year-old female during active right-arm elevation.

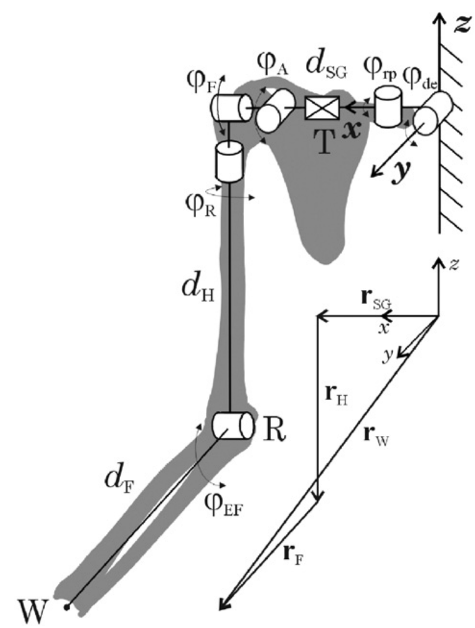

Fig. 1. Upper-arm kinematic model and calculated wrist vector $\mathbf{r}_{\mathrm{W}}$.

The upper-arm model does not replicate the arm's anatomical structure; it demonstrates the spatial motion characteristics of the reference point, W, on the wrist as the center between the *process styloideus ulnae* and the *process styloideus radii*. The model thus includes three rigid segments represented with: the SG vector, $\mathbf{r}_{\mathrm{SG}}$; the humerus vector, $\mathbf{r}_{\mathrm{H}}$; and the forearm vector, $\mathbf{r}_{\mathrm{F}}$. The origin of the reference coordinate is in the intersection of the medial-lateral axis through the center of the glenohumeral joint and the anterior-posterior axis through the sterna (Fig. 1).

In order to obtain the ARW effectively, we modeled the upper-arm with an emphasis on the SG's kinematics. The shoulder complex model consists of an inner and an outer shoulder joint. The inner shoulder joint has two perpendicular rotations and one translation (Fig. 1). The depression/elevation, φ_{de}, is a rotation of the SG about the y axis ($\mathbf{R}_{\mathrm{de}}$) and the retraction/protraction, φ_{rp}, is a rotation about the z-axis ($\mathbf{R}_{\mathrm{rp}}$). The outer shoulder joint has three perpendicular rotations, with the axes intersecting in the center of the glenohumeral joint. The humeral elevation through the adduction/abduction, φ_{A}, is a rotation about the y axis ($\mathbf{R}_{\mathrm{A}}$), the retroflexion/flexion, φ_{F}, is a rotation about the x axis ($\mathbf{R}_{\mathrm{F}}$), and the internal/external rotation, φ_{R}, is a rotation about the z axis ($\mathbf{R}_{\mathrm{R}}$). The elbow joint is considered as

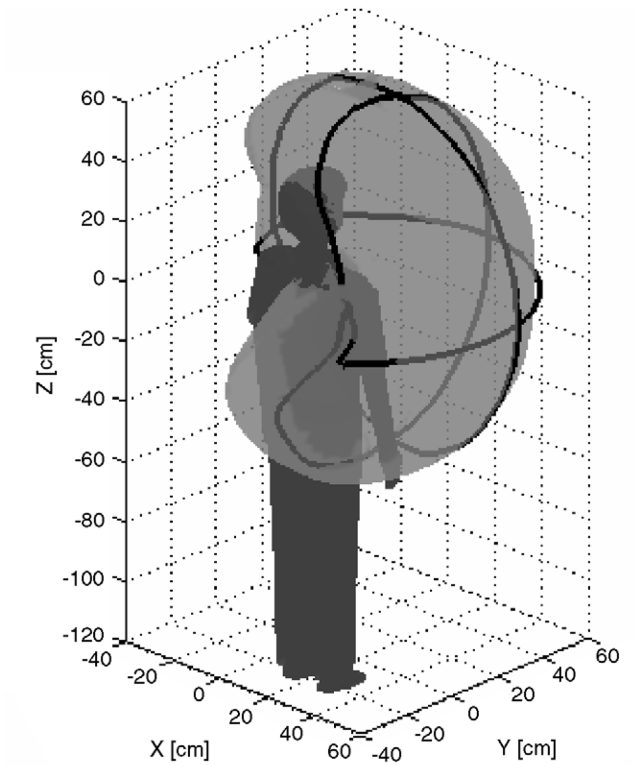

φ_{Fmin}	φ_{Fmax}	φ_{Amin}	φ_{Amax}	φ_{Rmin}	φ_{Rmax}
−60°	170°	−10°	170°	−60°	90°

volume
615.7 dm^3 ± 55.7dm^3

Fig. 2. Shoulder's RoM of healthy right arm ($H = 170$ cm), computed volume, comparison of calculated and measured ARW.

an uniaxial joint connecting the forearm with the humerus. Its extension/flexion is a rotation about the x-axis ($\mathbf{R}_{EF}$). The radioulnar joint (supination/pronation) is not included in the model since it does not influence the spatial position of the wrist.

The position of the wrist point, W, is calculated by the equation:

$$\mathbf{r}_W = \mathbf{R}_{de}\mathbf{R}_{rp}\mathbf{T} \cdot \mathbf{r}_{SG} + \mathbf{R}_A\mathbf{R}_F\mathbf{R}_R \cdot (\mathbf{r}_H + \mathbf{R}_{EF} \cdot \mathbf{r}_F), \qquad (2.1)$$

where all $\mathbf{R}$ represent the rotation matrixes about each defined axis for a defined angle, $\mathbf{T}$ as a translation represents the SG's length changes, and $\mathbf{r}$ are the arm-segment vectors. All the dependencies (Eqs. ((A.1)–(A.8)) are taken into consideration (see Appendix A).

2.2. Arm-reachable workspace calculation

The input data for the calculation of the arm-reachable workspace (ARW) are the measured shoulder RoM as joint limits. Relative to the height of the subject, H, the segments of the arm are normalized in accordance to the anthropometric table (Winter, 1990).

The procedure for determining the workspace has a number of stages. The first stage is to compute the set of points that can be reached by the wrist. This computation involves four nested loops, each associated with one joint angle. The first three loops represent the orientation of the humerus in terms of the outer shoulder-joint angles. The resolution is set to 5° for all the joint angles, corresponding to the data error of the input measurement. Within these outer shoulder-joint angles the inner shoulder-joint dependencies (Eqs. (A.5)–(A.7)) correlate with the SG's position. The last inside loop is the elbow extension/flexion angle. The procedure is repeated until all the ranges of the joint angles are calculated. The position $\mathbf{r}_W$ (Eq. (2.1)) is computed and stored as a 3D vector. In the next stage, the collisions between the segments of the arm (humerus and forearm) and the body (head, neck and trunk) have to be taken as obstacles. If an arm segment intersects the body during the computation, the related position of the wrist is eliminated as impossible.

The ARW outlined cube is divided up into a volume of n^3 smaller cubes for the volume calculation, where n is a reasonably limited resolution. The cubes that contain at least one point $\mathbf{r}_W$ represent the ARW volume, V. In order to increase the accuracy, the cubes forming the surface of the workspace are broken into eight smaller cubes with half the edge length of the original cubes. In every iterative step, the workspace volume, V, and the volume of cubes on the surface, V_S, are computed. The procedure ends when the relative error (V_S/V) is smaller than a prescribed value (0.1). For the graphical presentation the surface is determined, and in the last stage the ARW surface is smoothed. The computed ARW is presented in Fig. 2.

2.3. Measurement of the arm-reachable workspace

The ARW was measured on the healthy right arm of a 25-year-old female subject ($H = 170$ cm). The maximum wrist trajectory (i.e., reach) was drawn in the anatomical planes: the frontal, the sagittal and the horizontal. The measurements were carried out with an emphasis on the extreme angular range of the SG and no spine-rotation contribution to the extent of the arm's reach. These trajectories are used for a comparison with the ARW calculated on the basis of the upper-arm model (Fig. 2).

2.4. Measurement of the shoulder's RoM on the patient

To determine the extent of a shoulder injury in physiotherapy the passive shoulder's RoM was measured on the involved (left) arm of a 43-year-old female (158 cm, 62 kg) with a diagnosed frozen shoulder. The

Table 1
Frozen-shoulder patient's passive RoM and calculated ARW volume

Date	φ_{Fmin} (deg)	φ_{Fmax} (deg)	φ_{Amin} (deg)	φ_{Amax} (deg)	φ_{Rmin} (deg)	φ_{Rmax} (deg)	Volume (dm^3)
8.1.02	–30	105	–0	50	–35	5	$V_1 = 97.6$
22.1.02	–35	110	–0	60	–45	5	$V_2 = 142.5$
11.3.02	–40	115	–0	65	–50	5	$V_3 = 179.3$
25.3.02	–45	125	–5	75	–60	5	$V_4 = 240.9$
29.10.02	–55	135	–5	95	–70	15	$V_5 = 300.7$
6.11.02	–55	135	–5	95	–70	20	$V_6 = 305.7$

RoM was measured at the beginning, during and at the end of the patient's shoulder-pain treatment (Table 1).

3. Results

3.1. Evaluation of the arm-reachable workspace

The measured ARW is depicted in Fig. 2 as the maximum wrist trajectory in all three anatomical planes. It is elliptically elongated in specific directions. In the frontal plane the wrist trajectory shows the biggest extent above the head (i.e., superior ARW). It also shows the lowest extent in the area down and to the opposite side from the arm (i.e., anterior-inferior-opposite lateral ARW). In the sagittal and horizontal planes the extent is the biggest in front of the body (i.e., anterior ARW), while it is out of reach behind the body above (i.e., posterior-superior ARW). This area is reachable for the arm only with the contribution of spine rotations. The calculated ARW is in general agreement with the measured one (Fig. 2).

3.2. An evaluation of the upper-arm functioning using reachable workspace

The pattern of the measured unilateral passive shoulder's RoM recovery is evident during the frozen-shoulder patient's treatment (Table 1). The calculated ARW volume of the involved side was 97.6 dm^3 at the beginning (Table 1). During treatment volume increased in proportion to the whole RoM parameters, i.e., this evaluation provided a more general insight to the patient's improvements. The difference between the initial and final state of the patient was 208.1 dm^3. However, the calculated volume was only one evaluation tool; the shape of the ARW is also significant.

The ARW graphical envelope makes it possible to envisage the shape around the patient's body. Fig. 3 shows the ARW before V_1, some phases during V_2, at V_4, and at the end of the treatment, V_6. The progress during the rehabilitation is obvious.

The advantage of the ARW's transparent envelope is used when observing one space in another during an objective comparison. Fig. 4 shows a comparison of the ARW at the beginning and at the end of the treatment. This enables physiotherapists to accurately assess upper-arm functioning, measure progress and motivate patients. In this way the doctor and the patient can have a direct insight into the progress by making comparisons during the therapy.

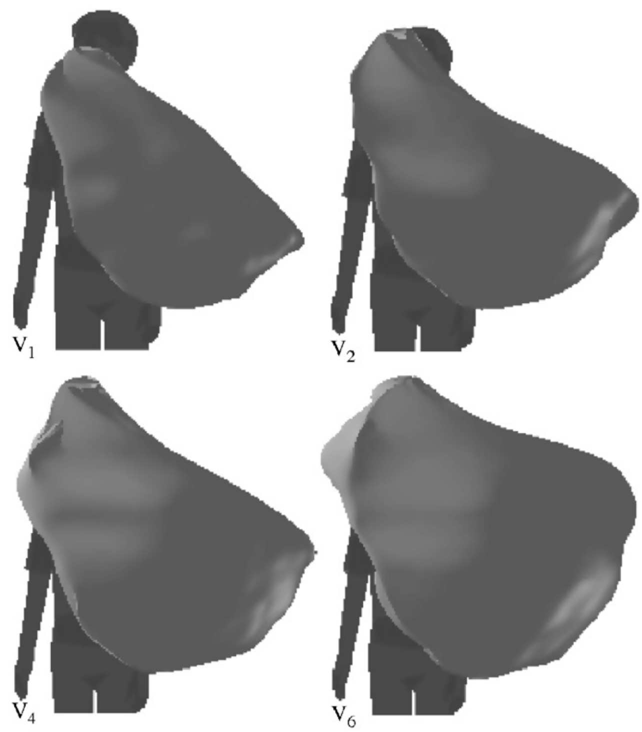

Fig. 3. ARW at the beginning (V_1), during (V_2, V_4) and at the end (V_6) of frozen-shoulder patient's treatment ($H = 158$ cm).

4. Discussion

The calculated ARW yields the upper-arm range, where all the positions of the wrist in space without a definition of the orientation of the hand are allowed. The hand can be oriented in different directions at the same point of the ARW due to the forearm supination/pronation. Additionally, the same point of the ARW can be reached with different compositions of the arm segments due to the redundancy in the arm system.

Fig. 4. Comparison of the ARW at the beginning (V_1) and at the end (V_6) of frozen-shoulder patient's treatment.

The advantage of our upper-arm kinematic model is that it considers the SG's kinematics, which gives a more exact ARW than the models from previous studies. The comparison of the volume results with previous studies shows that the ARW's volume with three rotations in the glenohumeral joint and one in the elbow (Savić, 1990) gives a smaller volume value (503.1 dm^3). The shape of this ARW is too spherical, as a very rough approximation. The model with a two additional rotations in the SG (Lenarčič and Umek, 1994) gives a bigger volume (690.5 dm^3), because the SG's angular motion range is considered as a constant. The shape is thus expanded with a larger convex hull. In our model the emphasis is on the precise kinematics of the SG. The volume of the presented upper-arm model (Fig. 1) is between both approximations, and the shape correctness was confirmed with the measurement (Fig. 2). The superior, anterior, inferior and both lateral regions agree exactly. The calculated ARW is in total agreement with wrist trajectories in the frontal and horizontal planes. The calculated ARW has a bigger extent than that measured only posterior in the sagittal plane. The reason is the performance of the measurement where the elbow positioning on the other side of the solid measuring plane is not possible.

The strength of an upper-arm model is at least partially based upon the ease of collection of input data. Therefore, the input data to the assistive tool for the ARW calculations are the measured shoulder's RoM, which are manually measured in physiotherapy. These parameters vary considerably among individuals, who may be different in terms of age, injuries or illness. They can also vary for the same individual, if measured passively or actively. Generally, the passive ranges of shoulder motion are bigger than the active ranges. Each measurement can be used clinically for a calculation of the ARW and a relevant comparison. In this way the measurements can be used to follow the improvement in the patient's ARW graphically (shape) and numerically (volume).

The likely most relevant outcome parameter of the model is the calculated workspace volume. It seems natural that an ARW with a larger volume is better than one with a smaller volume. We should also take into account that the arm-workspace volume depends on the individual's height.

Note that the workspace volume is only one of possible parameters associated with the functioning of the upper-arm. Other indices, such as the workspace shape and also the location of the workspace relative to the body, have to be used. The main advantage of the use of the ARW is the visualization that enables an easy, more complete, uniform and objective assessment. This helps to plan and control the rehabilitation procedure for patients with shoulder pathology.

The presented evaluation tool also enables a direct and practical comparison of the involved (disordered) arm to the uninvolved (healthy) one. The uninvolved ARW can be inverted and superimposed to the involved-hand side for the direct observation of the arm's disability (i.e. deficit).

Objective measurements, effective interpretations, visualizations and evaluations are also of crucial importance in advanced ergonomic and rehabilitation engineering. The motion of the human upper extremity is three dimensional and very difficult to evaluate and interpret. The ARW can anticipate the subject's kinematic functioning of the arm. For a more complete clinical upper-arm evaluation the result of the ARW should also include activities associated with daily living as well as incorporating force limitations.

5. Conclusion

An upper-arm model with an emphasis on the SG's kinematics was used to establish a database of wrist-motion range in the form of the ARW. The input data were taken from a standard evaluation procedure in physiotherapy. The arm-reachable workspace can be quantified in terms of its volume, and its main advantage is the ease of visualization. The obtained results can be used to predict and evaluate the abilities of the human upper extremity in different environments.

Acknowledgements

This project was supported by the Slovenian Ministry of Education, Science and Sport. The authors would like to thank the Institute for Rehabilitation of the Republic of Slovenia for its cooperation.

Appendix A. Limits of rotations in the kinematic upper-arm model

The upper-arm model includes simple rotations about fixed axes (Fig. 1). Basically, in the outer shoulder joint it is assumed that the limits of elevation through the adduction/abduction angle, $\varphi_{A,}$ are independent, so its range is

$$\varphi_A = [\varphi_{A\min}, \varphi_{A\max}]. \tag{A.1}$$

The limits of the elevation through retroflexion/flexion, φ_F, vary (Lenarčič and Umek, 1994):

$$\varphi_F = [\varphi_{F\min} + \varphi_A/3, \varphi_{F\max} - \varphi_A/6]. \tag{A.2}$$

The limits of the internal/external rotation, φ_R, vary within the following values (Lenarčič and Umek, 1994):

$$\varphi_R = [\varphi_{R\min} + 7\varphi_A/9 - \varphi_F/9 + 2\varphi_A\varphi_F/810, \\ \varphi_{R\max} + 4\varphi_A/9 - 5\varphi_F/9 + 5\varphi_A\varphi_F/810]. \tag{A.3}$$

The rotations of the outer joint have the primary function of the shoulder complex for positioning of the humerus in space. The elevation angle of the humerus is

$$\varphi = \arccos(\cos\varphi_A \cos\varphi_F), \tag{A.4}$$

with the additional condition: $\varphi \geqslant 0$ anteriorly and $\varphi < 0$ posteriorly.

The SG's positioning is mathematically added for every position of the humerus. The distance between the centre of the outer joint from the origin point is changing during humeral elevation. It is imitated in the model with the changing length of the SG vector. The length of the SG contracts as a quadratic function, depending on the unilateral elevation angle of the humerus (Klopčar and Lenarčič, 2005)

$$d_{SG}/d_o = -1.6 \cdot 10^{-5}\varphi^2 + 3 \cdot 10^{-4}\varphi + 1, \tag{A.5}$$

with respect to the initial condition of the SG's base position ($d_{SG}/d_o = 1$, $\varphi_{de} = \varphi_{rp} = 0^\circ$) in the reference position of the arm ($\varphi = 0^\circ$).

On average, the SG's angular motion range depending on unilateral humeral elevation is a quadratic function for the depression/elevation inclinations, φ_{de}, (Klopčar and Lenarčič, 2005)

$$\Delta\varphi_{de} = [0.0021\varphi^2 - 0.04\varphi - 14^\circ, \\ 0.0013\varphi^2 - 0.03\varphi + 30^\circ] \tag{A.6}$$

and for the retraction/protraction inclinations, φ_{rp},

$$\Delta\varphi_{rp} = [-0.0012\varphi^2 + 0.15\varphi - 26^\circ, \\ -0.0022\varphi^2 + 0.15\varphi + 30^\circ]. \tag{A.7}$$

The limits of the elbow extension/flexion angle, φ_{EF}, are assumed to be constant:

$$\varphi_{EF} = [\varphi_{EF\min}, \varphi_{EF\max}], \tag{A.8}$$

where $\varphi_{EF\min}$ is –90° and $\varphi_{EF\max}$ is 60° for a healthy elbow. In all equations the angles are expressed in degrees.

References

Constant, C.R., Murley, A.H., 1987. A clinical method of functional assessment of the shoulder. Clinical Orthopaedics 214, 160–164.

Doorenbosch, C.A.M., Mouritis, J.J.M., Veeger, H.E.J., Harlaar, J., van der Helm, F.C.T., 2001. Determination of the axes of rotation about the shoulder during elevation. Journal of Orthopaedic & Sports Physical Therapy 31, 133–137.

Dvir, Z., Berme, N., 1978. The shoulder complex in elevation of the arm: a mechanism approach. Journal of Biomechanics 11, 219–225.

Engin, A.E., Peindl, R.D., 1987. On the biomechanics of human shoulder complex—I. Kinematics for determination of the shoulder complex sinus. Journal of Biomechanics 20, 103–117.

Engin, A.E., Tümer, S.T., 1989. Three-dimensional kinematic modelling of the human shoulder complex—part I: physical model and determination of joint sinus cones. Journal of Biomechanical Engineering 111, 107–112.

van der Helm, F.C.T., 1997. A three-dimensional model of the shoulder and elbow. In: Proceedings of the First Conference of the International Shoulder Group. Delft University of Technology.

Klopčar, N., Lenarčič, J., 2005. Bilateral and unilateral shoulder girdle kinematics during humeral elevation. Clinical Biomechanics, in press.

Lenarčič, J., Umek, A., 1994. Simple model of human arm reachable workspace. IEEE Transactions on Systems, Man, and Cybernetics 24, 1239–1246.

Maurel, W., Thalmann, D., 2000. Human shoulder modeling including scapulo-thoracic constraint and joint sinus cones. Computers and Graphics 24, 203–218.

Norkin, C.C., White, D.J., 1985. Measurement of joint motion: a guide to gonimetry. F. A. Davis Company, Philadelphia.

Savić, S., 1990. Mathematical model and workspace of human arm—a study for rehabilitation. M.Sc. thesis, University of Ljubljana, Faculty of Electrical Engineering and Computer Sciences, Ljubljana.

Wang, X., Maurin, M., Mazet, F., Maia, N.D.C., Voinot, K., Varriest, J.P., Fayet, M., 1998. Three-dimensional modelling of the motion range of axial rotation of the upper arm. Journal of Biomechanics 31, 899–908.

Winter, D.A., 1990. Biomechanics and motor control of human movement. Wiley-Interscience Publication, University of Waterloo, pp. 51–74.